치의학박사 학위논문

Peritumoral bone change in oral squamous cell carcinoma: Correlation of imaging features with histopathological findings

구강편평세포암종의 주변 골 변화: 영상 특성 및 조직병리학적 상관관계 분석

2018 년 2 월

서울대학교 대학원

치의과학과 영상치의학 전공

조 규 동

Abstract

Peritumoral bone change in oral squamous cell carcinoma: Correlation of imaging features with histopathological findings

Gyu-Dong Jo, DDS

Department of Oral and Maxillofacial Radiology,

Graduate School, Seoul National University

(Directed by Prof. Kyung-Hoe Huh, DDS, MSD, PhD)

Purpose

When oral squamous cell carcinoma (OSCC) invades the jaw bone, increased attenuation on computed tomography (CT) or pathologic signal intensity (SI) on magnetic resonance (MR) images is frequently observed in the remaining margin, which makes it difficult to determine the extent of tumor invasion.

The aims of the current study were, in OSCC patients with mandibular bone invasion 1) to assess the prevalence of underlying bone change on preoperative CT and MR images, 2) to investigate the relationship between underlying bone change and tumor aggressiveness, and 3) to analyze the area of underlying bone change on histopathology slides through radiologic-histopathologic correlation.

Materials and Methods

This study consisted of 137 subjects who underwent mandibulectomy to treat OSCC between September 2009 and December 2016. Preoperative CT and MR images were evaluated by two oral and maxillofacial radiologists to assess the prevalence of underlying bone change. In addition, correlations of underlying bone change with each of radiologic findings (type of bone invasion, depth of bone invasion, tumor size), histopathologic findings (TN stage, degree of malignant cell differentiation), and clinical finding (recurrence) were analyzed.

In 18 subjects who underwent mandibulectomy after January 2016, serial section slides of resected specimens were prepared and a blinded oral pathologist analyzed the underlying bone change area on histopathology slides. Histopathologic features (presence of malignant tumor cell, alteration of trabecular bone, fibrosis of marrow space, inflammatory cell infiltration) were evaluated and pattern of peritumoral bone change was classified based on these.

Results

In preoperative imaging analysis, 69.6% CT and 90.9% MR showed underlying bone sclerosis and pathologic SI in underlying bone marrow. Those with underlying bone change had a significantly aggressive invasion type, deeper invasion depth, and bigger tumor size.

Histopathologic pattern of peritumoral bone change was grouped into three patterns: four cases of sclerosis dominant, ten cases of fibrosis dominant, and four cases of invasion dominant patterns. In the cases classified as sclerosis dominant and fibrosis dominant patterns, no malignant tumor cell infiltration was found on histopathology slides while underlying bone changes were observed on preoperative images.

Conclusion

Underlying bone change is often accompanied by OSCC in forms of sclerosis or pathologic SI of bone marrow. It is very important to distinguish and differentiate between bone invasion by OSCC and resultant surrounding bone change. This will help to determine the bone margin of surgical resection in patients with OSCC.

Keywords: Carcinoma, Squamous Cell; Mandible; Tomography, X-ray Computed radiograph, Magnetic Resonance Imaging

Student number: 2015-31271

Contents

I. Introduction

Oral squamous cell carcinoma (OSCC) is one of the most aggressive malignancies and accounts for more than 90% of all oral and oropharyngeal caner.[1] OSCC originating from gingival mucosa, which is the second most common site for OSCC after the tongue, frequently invades the mandible due to close proximity to underlying bone.[2,3] Therefore, it is frequently graded as stage T4 at presentation and consequently treatment of the lesion includes resection of underlying bone. In that point, recent study suggested that gingival OSCC should be looked upon with special attention and be handled separately from other subsites in the oral cavity.[4]

Composite resection of tumor mass with en bloc resection of underlying bone is the main treatment modality for gingival OSCC.[5] Obtaining clear resection margin that included healthy surrounding tissue is the best way to minimize the risk for local recurrence.[6] Even when considering this point, the current treatment tends to include extensive resection without histopathological evidence. Segmental resection rather than marginal resection is preferred when there is a clinical evidence of gingival mucosa invasion and adhesion to the bone but no radiologic evidence of bone resorption.

For improved quality of life, preserving the inferior border of the mandible is very important, if oncologically safe. Preserving the mandibular continuity using marginal mandibulectomy has two advantages. First, it minimizes morphological changes in terms of esthetic and resultant psychological

aspects. Second, it avoids dislocation of the temporomandibular joint (TMJ) in terms of functional aspects.

Computed tomography (CT) and magnetic resonance (MR) images are commonly used to evaluate the presence and the extent of mandibular invasion in patients with OSCC. Based on the extent of mandibular invasion, either a marginal or a segmental mandibulectomy is determined.[7,8] In clinical setting, underlying bone change on CT and MR images has been observed for a number of OSCC cases. It results in indistinct tumor margins and overestimation of mandibular invasion (Figure 1). Determining the margin of surgical resection becomes difficult because radiologists are not certain about the presence of malignant tumor cells in the area of underlying bone change. It leaves a question whether the change was caused by tumor cell infiltration, or it is just reactive change and there is no tumor cell in the underlying bone.

There have been few studies on the bone change adjacent to tumor mass. A study revealed that nearly 60% of nasopharyngeal carcinoma patients had developed sclerosis in pterygoid process adjacent to tumor mass.[9] Although the cause of pterygoid process sclerosis was uncertain, they suggest that this change would reflect the bone's response to the presence of nearby tumor. Another study showed that the presence of sclerosis in the mandible might be an early indication of microscopic disease and should increase suspicion of mandibular invasion of OSCC.[10]

Considering these previous findings, we hypothesized that bone destruction by OSCC would always be accompanied by underlying bone

change associated with tumor-bone interactions, but there would be no malignant tumor cells in the area of the underlying bone change.

The aims of the current study were, in OSCC patients with mandibular bone invasion 1) to assess the prevalence of underlying bone change on preoperative CT and MR image, 2) to investigate the relationship between underlying bone change and tumor aggressiveness and 3) to analyze the area of underlying bone change on histopathology slides through radiologic-histopathologic correlation.

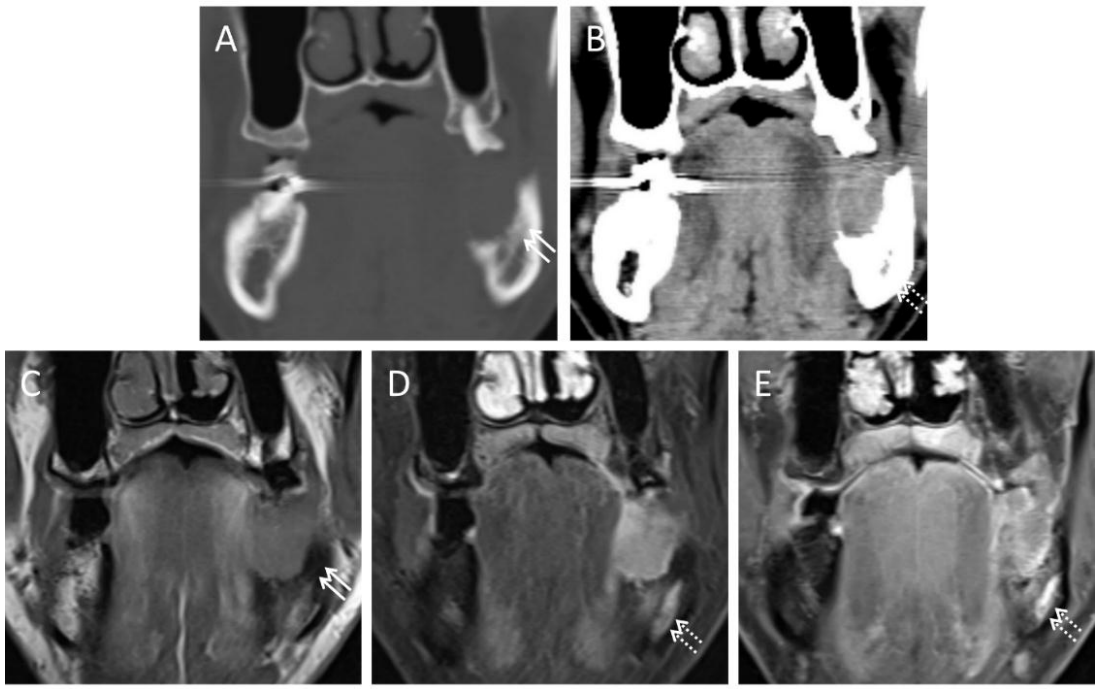

Figure 1. Underlying bone change (A) CT image with bone setting shows underlying bone sclerosis (arrow). (B) CT image with soft tissue setting shows increased attenuation of underlying bone marrow (dashed arrow). (C) T1WI shows low SI of underlying bone (arrow). (D) fat suppressed T2WI shows high SI of underlying bone marrow (dashed arrow). (E) contrast enhanced T1WI shows enhancement of underlying bone marrow (dashed arrow).

II. Materials and Methods

This study was approved by the Institute Review Board of Seoul National Dental Hospital (IRB007/01-15).

To verify the hypothesis, we 1) evaluated the prevalence of underlying bone sclerosis on CT images and pathologic signal intensity (SI) of underlying bone marrow on MR images, and 2) assessed the correlation between underlying bone change and other radiologic, histopathologic, clinical variables considered as a predictor of tumor aggressiveness. Also we 3) analyzed the area of underlying bone change on histopathology slides through radiologic-histopathologic correlation.

This study consisted of 213 subjects who underwent mandibulectomy to treat OSCC between September 2009 and December 2016. Subjects with recurrence, a lesion arising from the area other than the gingiva (e.g., buccal mucosa, lip, tongue, floor of mouth, or pharynx), or who received preoperative radiotherapy or chemotherapy were excluded. In addition, subjects were excluded when their images had severe artifact and unable to evaluate underlying bone. Finally, 76 subjects were excluded.

1. Prevalence of underlying bone change

Total 137 subjects' preoperative CT and MR images were analyzed. All images were evaluated by consensus of two experienced oral and maxillofacial radiologists using the picture archiving and communication system (Infinitt PACS, Infinitt Healthcare, Seoul, Korea).

1.1. Preoperative CT image analysis

Underlying bone was defined as the bone marrow space directly beneath the deepest bone margin infiltrated by tumor mass. Sclerosis was defined as increased attenuation of medullary cavity on bone window CT images. The presence of underlying bone sclerosis was evaluated as either present or absent and the prevalence of underlying bone sclerosis was calculated. Underlying bone sclerosis was evaluated further in terms of the degree and extent.

The degree of underlying bone sclerosis was assessed qualitatively as well as quantitatively. Qualitatively, the degree of underlying bone sclerosis was categorized as being either absent, subtle, or prominent in comparison with the corresponding region on the contralateral side of the mandible. Quantitatively, 10 mm^2 circular region of interest (ROI) was set and average Hounsfield unit (HU) was measured in underlying bone and the corresponding region on the contralateral side of the mandible. The difference of HU values between the two sets of measurement was named "The degree of underlying bone sclerosis"

The extent of underlying bone sclerosis was evaluated qualitatively as follows: 0, no sclerosis; 1, sclerosis was present but did not extend over the mandibular canal; 2, sclerosis was present and extended over the mandibular canal.

1.2. Preoperative MR image analysis

Pathologic signal intensity (SI) of underlying bone marrow was defined as low SI on T1-weighted image (T1WI), high SI on fat suppressed T2-weighted image (T2WI) and enhancement on contrast enhanced T1WI in comparison with the corresponding region of the contralateral side of the mandible. The presence of pathologic SI was evaluated as either absent or present and the prevalence of pathologic SI was calculated separately for each sequence. Pathologic SI was evaluated further in terms of the extent.

The extent of pathologic SI was also recorded as follows: 0, normal SI; 1, pathologic SI was present but did not extend over the mandibular canal; 2, pathologic SI was present and extended over the mandibular canal.

1.3. Agreement between CT and MR imaging findings

The agreement between CT and MR imaging findings on underlying bone change was measured with kappa statics (0, agreement is a random effect; less than 0.20, poor agreement; 0.21–0.40, fair agreement; 0.41–0.60, moderate agreement; 0.61–0.80, substantial agreement; and 0.81–1.00, excellent agreement).

2. Correlation between underlying bone change and tumor aggressiveness

Radiologic, histopathologic, clinical variables considered as a predictor of tumor aggressiveness were analyzed. Correlation between underlying bone change and theses variables were statistically evaluated. A P value of <.05 was considered statistically significant.

Preoperative CT images were evaluated by two oral and maxillofacial radiologists. Pathology reports and electronic medical records were reviewed by an oral and maxillofacial radiologist who participated in imaging analysis. All statistical analyses were performed by using SPSS version 22 (IBM Corporation, Armonk, NY, USA).

2.1. Preoperative CT image analysis

The radiologic type of bone invasion was evaluated and categorized as either cortical invasion, medullary invasion with a smooth margin, or medullary invasion with an irregular margin. A smooth margin was defined as a well-defined border with a narrow transition zone and no residual bone behind the border. An irregular margin was defined as an ill-defined border with a wide transition zone and finger like extension into the surrounding bone.[11]

In addition, the depth of bone invasion was measured as the actual distance between alveolar crest and the deepest margin of bone destruction on

coronal view. The tumor size was measured by the longest dimension in axial, coronal, and sagittal views.

2.2. Histopathologic and clinical analysis

Pathology reports were reviewed and degree of differentiation (well, moderately, poorly differentiated), T stages (T1, T2, T3, T4), N stages (N0, N1, N2), and pathologic TNM stages (I, II, III, IV) were recorded.

Electronic medical records were also reviewed for matter of recurrence.

2.3. Correlation between underlying bone change and tumor aggressiveness

Table 1 shows list of all the assessment items in terms of underlying bone change and tumor aggressiveness.

The difference in prevalence of underlying bone change between cortical invasion group and medullary invasion group was evaluated using Chi-square tests for independence and post-hoc analysis.

Association between the qualitatively assessed degree of underling bone sclerosis and the categorical variables (radiologic type of bone invasion, degree of differentiation, T stages, N stages, pathologic TNM stages, matter of recurrence) were evaluated using linear by linear association test. In addition, correlations between the extent of underlying bone sclerosis and the categorized variables were analyzed.

One-way ANOVA was used to estimate the difference in the quantitatively assessed degree of underlying bone sclerosis (HU value) among groups classified by radiologic bone invasion type.

Correlation between the quantitatively assessed degree of underlying bone sclerosis (HU value) and continuous variables (depth of invasion, tumor size) were evaluated using Pearson's correlation coefficient analysis.

3. Presence of malignant tumor cells in the area of underling bone change

To analyze the area of underlying bone change microscopically, serial section slides of resected specimens were prepared and evaluated. Among all 137 subjects, 18 subjects who underwent mandibulectomy after January 2016 were enrolled.

All histopathology slides were evaluated by a blinded and experienced oral pathologist.

3.1. Preoperative image analysis

Preoperative CT and MR image analysis was done in the previous analysis. Additionally, the presence of fluorodeoxyglucose (FDG) uptake in underlying bone was also evaluated on preoperative PET-CT images. The change was analyzed on the basis of degree of uptake on the contralateral side mandible.

3.2. Preparation of histopathology slides using postoperative cone beam computed tomography (CBCT) images of resected specimens

After the surgical resection, cone beam computed tomography (CBCT) of resected specimen was taken after 24 hours of fixation (Figure 2). After decalcification of the specimens, serial section slides were prepared perpendicularly to long axis of mandibular arch. It included the deepest region of bone destruction and the regions 4 mm anterior and posterior to it (Figure 3). CBCT images of the specimens were used when determining the

deepest region of bone destruction. It improved the accuracy in determining the region of interest for radiologic–histopathologic correlation.

3.3. Histopathologic analysis

Histopathologic type of bone invasion was recorded as either erosive type or infiltrative type, based on the morphology of tumor front. The erosive type was characterized by a broad and expansive tumor front with a sharp interface between tumor and bone. In contrast, the infiltrative type was composed of tumor cell nest with finger like projections along with an irregular tumor front.

The presence of malignant tumor cells was histopathologically evaluated on the three serially sectioned slides which included the region of deepest bone destruction and the regions 4 mm anterior and posterior to it. The alteration of trabecular bone, fibrosis of marrow space, and inflammatory cell infiltration were additionally assessed. Based on these findings, we newly named and classified “Histopathologic patterns of peritumoral bone change”.

3.4. Radiologic–histopathologic correlation

The relationship between radiologic and histopathologic findings were investigated.

Table 1. List of all the assessment items in terms of underlying bone change and tumor aggressiveness.

Underlying bone change		Tumor aggressiveness		
CT	MR	Radiologic	Histopathologic	Clinical
Degree of sclerosis (Qualitative)	Extent of pathologic SI	Type of bone invasion	Degree of differentiation	Recurrence
Degree of sclerosis (Quantitative, HU values)		Depth of bone invasion	T stage	
Extent of sclerosis		Tumor size	N stage	
			pTNM stage	

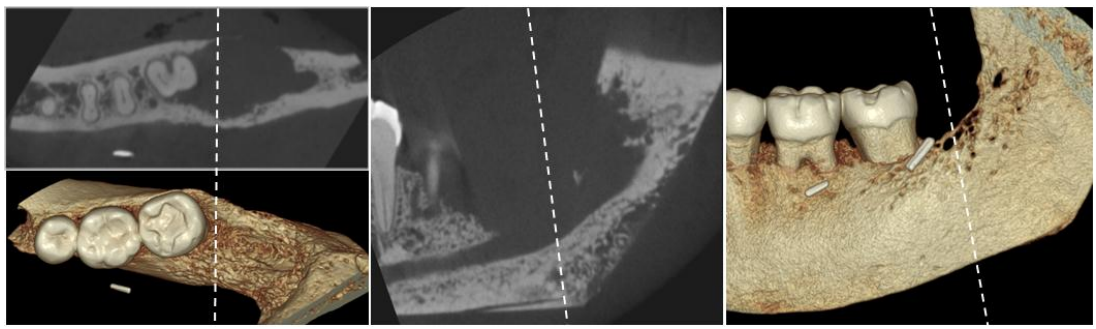

Figure 2. Post-operative CBCT images of resected specimen. Dashed line: the deepest region of bone destruction, and the sectioning plane for histopathology slides.

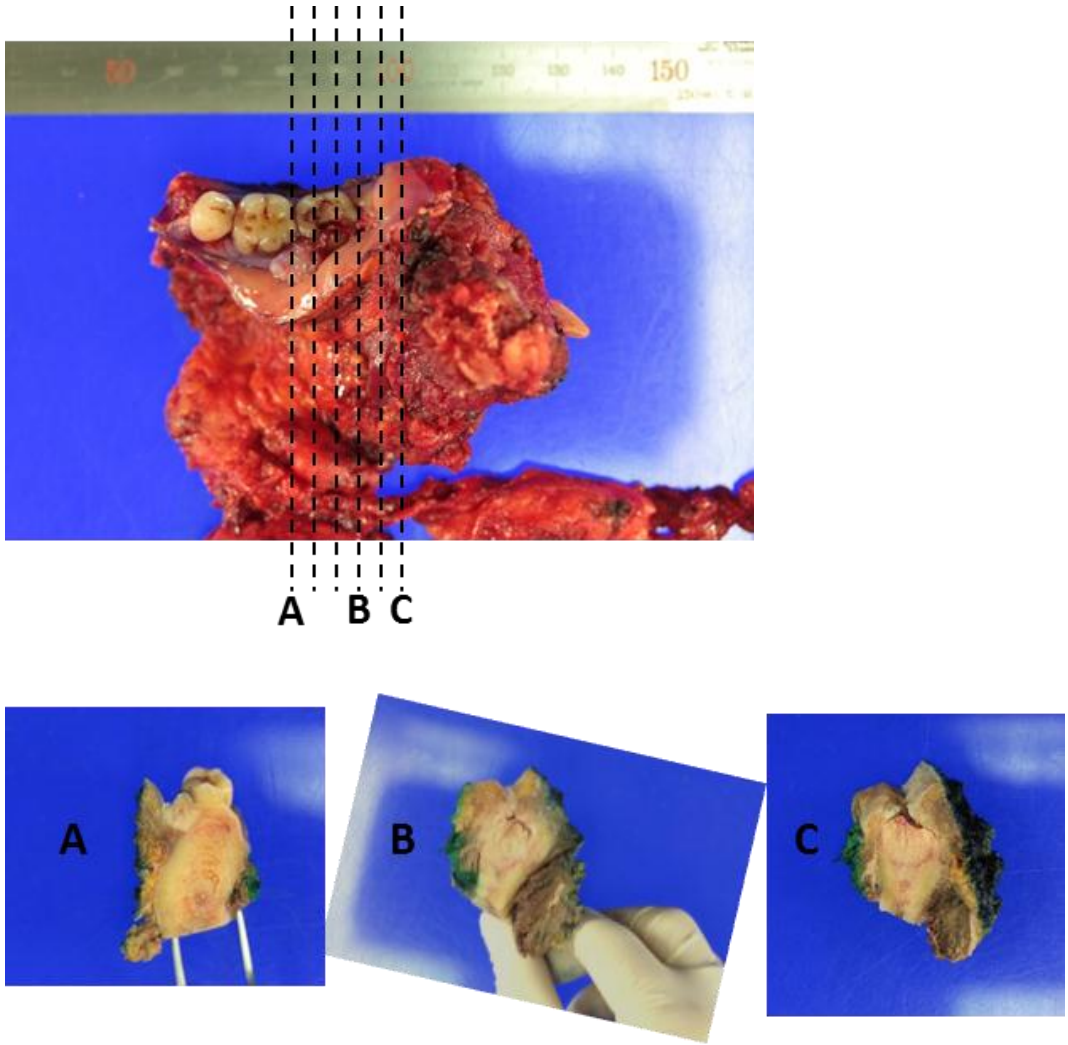

Figure 3. Serial section of the specimen. A: anterior to the deepest region, B: the deepest region of bone invasion, C: posterior to the deepest region

III. Results

1. Prevalence of underlying bone change

1.1. Preoperative CT image analysis

Of 137 cases, bone destruction had progressed to the inferior cortex of the mandible in 25 cases. These 25 cases were infeasible for further analysis because they lacked remaining bone marrow. The prevalence of underlying bone sclerosis was 69.6% (78 of 112) in patients with OSCC.

Qualitatively assessed the degree of underlying bone sclerosis was distributed as follows: 30.4% in absent, 44.6% in subtle, 25.0% in prominent. Mean of quantitatively assessed the degree of underlying bone sclerosis (HU values) was 438.5 (825.5 in underlying bone and 387.0 in the corresponding region on the contralateral side of the mandible).

The extent of underlying bone sclerosis was distributed as follows: 30.4% in no sclerosis, 42.9% in sclerosis not extended over the mandibular canal, 26.7% in sclerosis extended over the mandibular canal.

1.2. Preoperative MR image analysis

Of 137 cases included in CT evaluation, 13 cases were excluded in MR evaluation. Eight cases were not imaged with MR images. Either fat

suppressed T2WI or contrast enhanced T1WI sequence was missing in 5 cases.

On the T1WI, 77 cases (77.8%) showed low SI in the underlying bone marrow space. The low SI in 52 cases was limited to the alveolar bone, the other 25 cases showed low SI that extended to the basal bone.

On fat suppressed T2WI, 84 cases (84.8%) had high SI. There were 16 cases of high SI that was limited to the alveolar bone, 68 cases of high SI that extended to the basal bone.

On contrast enhanced T1WI, 84 cases (84.8%) showed enhancement. There were 17 cases of enhancement that was limited to the alveolar bone, and 67 cases of enhancement that extended to the basal bone.

Among the three sequences of T1WI, fat suppressed T2WI and contrast enhance T1WI, 90 cases (90.0%) and 69 cases (69.7%) had pathologic SI of underlying bone marrow observed in at least one sequence and all sequences respectively.

1.3. Agreement between CT and MR imaging findings

Table 2 shows the agreement between CT and MR findings. Excellent to substantial agreement were observed each between CT and T1WI, fat suppressed T2WI and contrast enhanced T1WI. The rest combinations showed fair to poor agreement.

Even when there was no clear observation of underlying bone sclerosis on CT image, pathologic SI of underlying bone was further observed on MR image. Among 36 cases with no observation of underlying bone sclerosis on CT, 5 cases showed pathologic SI on T1WI and 25 cases showed pathologic SI on fat suppressed T2WI or contrast enhanced T1WI.

2. Correlation between underlying bone change and tumor aggressiveness

2.1. Preoperative CT image analysis

The radiologic types of bone invasion were observed as follows: 31 cases (27.7%) of cortical invasion, 20 cases (17.9%) of medullary invasion with a smooth margin, 61 cases (54.5%) of medullary invasion with an irregular margin.

The mean depth of bone invasion was 7.4 mm and the mean tumor size was 27.7 mm.

2.2. Histopathologic and clinical analysis

The degree of differentiation was observed as follows: 86 cases of well differentiation, 24 cases of moderate differentiation, 0 cases of poor differentiation. 2 cases had no result.

T stage was observed as follows: 14 cases of T1, 26 cases of T2, 2 cases of T3, 60 cases of T4, 10 cases of none. N stage was observed as follows: 63 cases of N0, 11 cases of N1, 22 cases of N2, 16 cases of none. Regarding pathologic TNM stages, 8 cases observed as stage I, 19 as stage II, 6 as stage III, 69 as stage IV and 10 cases had none.

Recurrence was observed in 13 cases (11.6%).

2.3. Correlation between underlying bone change and tumor aggressiveness

The prevalence of underlying bone sclerosis was 82.7% (67 of 81) in patients with medullary invasion, but was 35.5% (11 of 31) in patients with only cortical invasion, indicating a significant increase in the prevalence of underlying bone sclerosis in patients with medullary invasion ($P<.05$). The medullary invasion group was 9.833 times more likely to have underlying bone sclerosis compared to the cortical invasion group (Odds ratio = 9.833). Presence of underlying bone sclerosis was more likely to be the medullary invasion group by 2.169-folds (Relative risk = 2.169).

Compared to cortical invasion group, medullary invasion group had significantly increased prevalence of pathologic SI on T1WI (Odds ratio = 5.556, Relative risk = 1.759), fat suppressed T2WI (Odds ratio = 7.262, Relative risk = 2.131), contrast enhanced T1WI (Odds ratio = 18.485, Relative risk = 3.671) ($P<.05$).

Increases in the degree and extent of underlying bone sclerosis were associated with aggressive radiologic type of bone invasion ($P<.05$) (Figure 4, Figure 5).

Of the 31 cases in the cortical invasion group, 21 had no underlying bone sclerosis. Subtle sclerosis that was limited to the alveolar bone was observed in the remaining 10 cases (Figure 6).

Of the 20 cases in medullary invasion with a smooth margin group, 14 had underlying bone sclerosis (Figure 7). There were 9 cases of subtle sclerosis that was limited to the alveolar bone, 2 cases of subtle sclerosis that included

the basal bone, and 3 cases of prominent sclerosis that was limited to the alveolar bone. None in this group had prominent sclerosis that included the basal bone.

Of the 61 cases in medullary invasion with an irregular margin group, 53 had underlying bone sclerosis (Figure 8). There were 18 cases of subtle sclerosis that was limited to the alveolar bone, 10 cases of subtle sclerosis that included the basal bone, 7 cases of prominent sclerosis that was limited to the alveolar bone, and 18 cases of prominent sclerosis that included the basal bone.

There was a significant difference in the degree of underlying bone sclerosis (HU value) among groups classified by radiologic type of bone invasion (P <.05) (Table 3). Cortical invasion group had lower HU value compared to medullary invasion group. There was no significant difference in HU values between medullary invasion with smooth margin group and medullary invasion with irregular margin group.

Increase in the degree of underlying bone sclerosis (HU) was significantly associated with increase in the invasion depth and tumor size (P<.05) (Table 4). However, when adjusted for tumor size, HU value did not increase according to invasion depth. On the other hand, HU value increased as tumor size increases when adjusted for invasion depth. Therefore, the degree of underlying bone sclerosis (HU) would have more significant association with tumor size than invasion depth.

No other data had a significant relationship with underlying bone change on preoperative images.

3. Presence of malignant tumor cells in the area of underling bone change

3.1. Preoperative image analysis

Of the 18 cases, 4 cases had bone destruction up to the inferior cortex of the mandible. These 4 cases were infeasible for further analysis because they lacked remaining bone marrow.

Underlying bone sclerosis was observed in 12 cases on CT images. Pathologic SI of underlying bone marrow was observed in 13 cases on MR images. Low SI on T1WI was observed in 11 cases. All these cases showed underlying bone sclerosis on CT images simultaneously. Ten cases showed high SI on fat suppressed T2WI and enhancement on contrast enhanced T1WI. Except one case, the majority of cases revealed no FDG uptake on PET-CT.

Regarding the radiologic type of invasion, 4 cases were classified as cortical invasion, 2 cases as medullary invasion with a smooth margin, 8 cases as medullary invasion with an irregular margin.

3.2. Histopathologic analysis

Regarding histopathologic type of bone invasion of the 18 cases, 6 cases were erosive and 12 cases were infiltrative type.

In the current study, we categorized peritumoral bone change further into three patterns: sclerosis, fibrosis, and invasion dominant (Figure 9). Of 18

cases, 4 cases were sclerosis dominant pattern, 10 cases were fibrosis dominant pattern, and 4 cases were invasion dominant pattern.

Sclerosis dominant pattern was only observed with erosive type. Loss of previous trabecular structure and dense sclerotic bone was observed. There were only few inflammatory cells and no malignant tumor cell was found.

Fibrosis dominant pattern was found in both erosive pattern and infiltrative type. Alteration of normal trabecular structure and fibrosis of inter-trabecular space was observed. Zone of fibrosis was defined as the vertical length of fibrosis from the interface of tumor and bone. The zone of fibrosis raged from 3 to 10 mm. Fibrosis dominant pattern had intermediate degree of inflammatory cell infiltration, which was in between sclerosis dominant pattern and invasion dominant pattern. There was no malignant tumor cell observed. Fibrosis dominant pattern showed three subtypes, 1) only fibrosis, 2) fibrosis with focal woven bone formation, and 3) desmoplasia which means dense fibrosis.

Invasion dominant pattern was seen only in infiltrative type. Tumor islands within the inter-trabecular space accompanied by severe inflammation were extensively observed. In addition, fibrosis in cancer tissue itself was also observed.

3.3. Radiologic-histopathologic correlation

Table 5 shows the relationship between radiologic and histopathologic findings of peritumoral bone change.

Sclerosis dominant pattern showed dense sclerosis on CT and low SI on T1WI (Figure 10). Fibrosis dominant pattern showed increased attenuation of marrow space on CT, high SI on fat suppressed T2WI, and enhancement on contrast enhanced T1WI (Figure 11, Figure 12). Invasion dominant pattern showed bone destruction to the inferior cortex of the mandible and no remaining bone marrow to be evaluated on preoperative images (Figure 13).

Important point is, isolated malignant tumor cell nest was not found in underlying bone for sclerosis and fibrosis dominant patterns.

Table 2. The degree of agreement between CT findings and MR findings on presence and extent of underlying bone change.

Presence	Kappa value	Strength of agreement	Extent	Kappa value	Strength of agreement
CT–T1	0.904*	Excellent	CT–T1	0.795*	Substantial
T2–En	0.728*	Substantial	T2–En	0.854*	Excellent
T1–T2	0.389*	Fair	T1–T2	0.148*	Poor
T1–En	0.389*	Fair	T1–En	0.148*	Poor
CT–T2	0.328*	Fair	CT–T2	0.133*	Poor
CT–En	0.328*	Fair	CT–En	0.133*	Poor

* $P < .05$

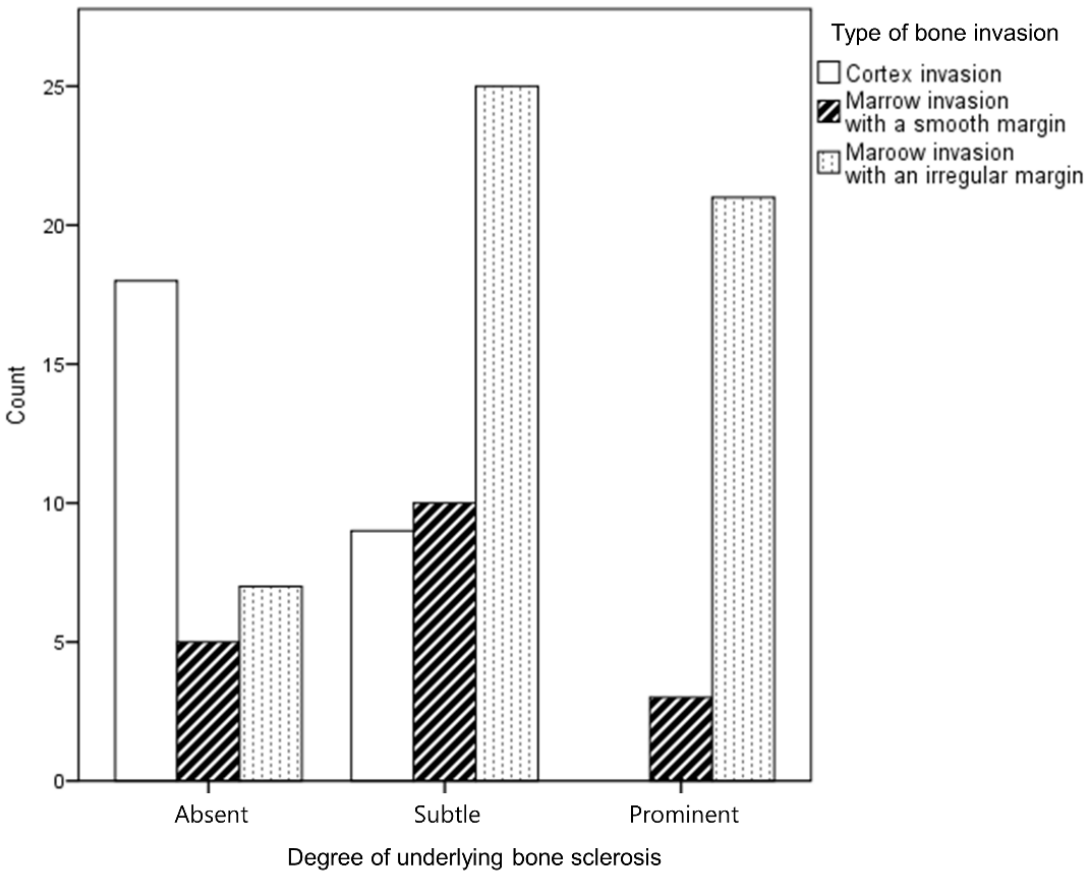

Figure 4. Degree of underlying bone sclerosis according to radiologic type of bone invasion. Increases in the degree of underlying bone sclerosis was significantly associated with aggressive radiologic type of bone invasion.

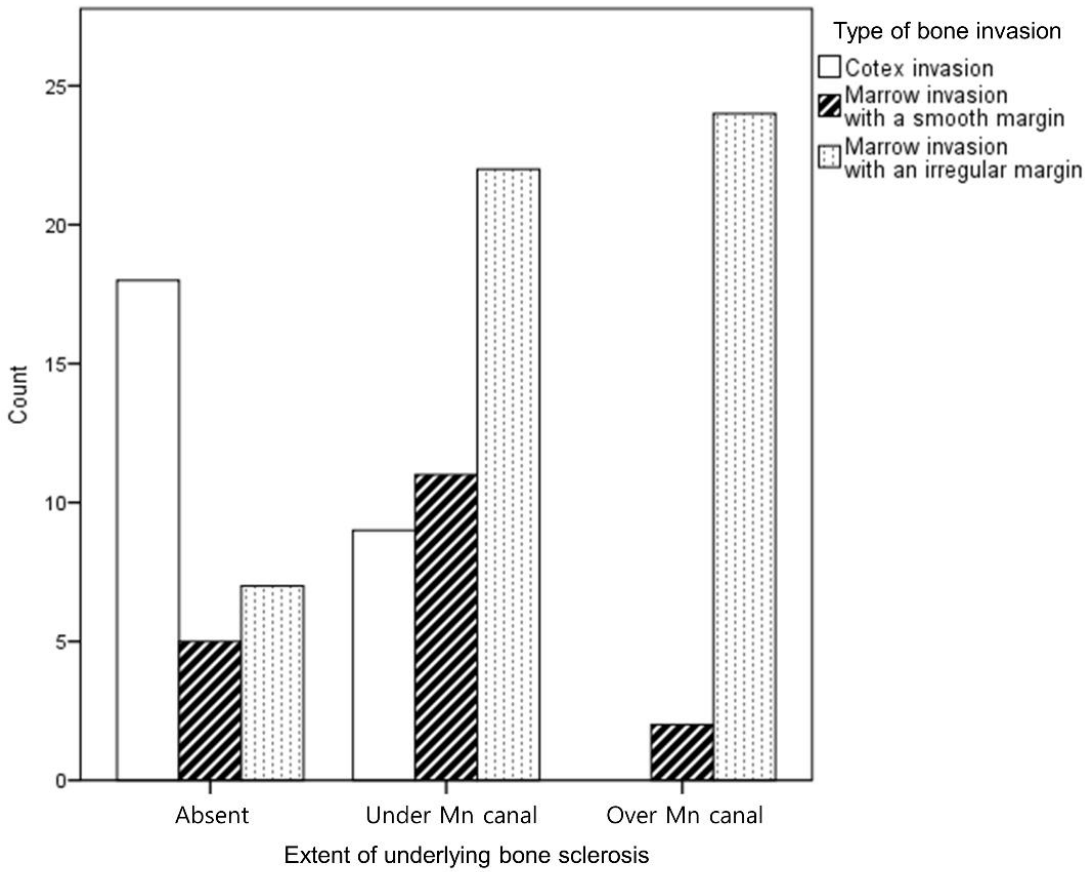

Figure 5. Extent of underlying bone sclerosis according to radiologic type of bone invasion. Increases in the extent of underlying bone sclerosis was associated significantly with aggressive radiologic type of bone invasion.

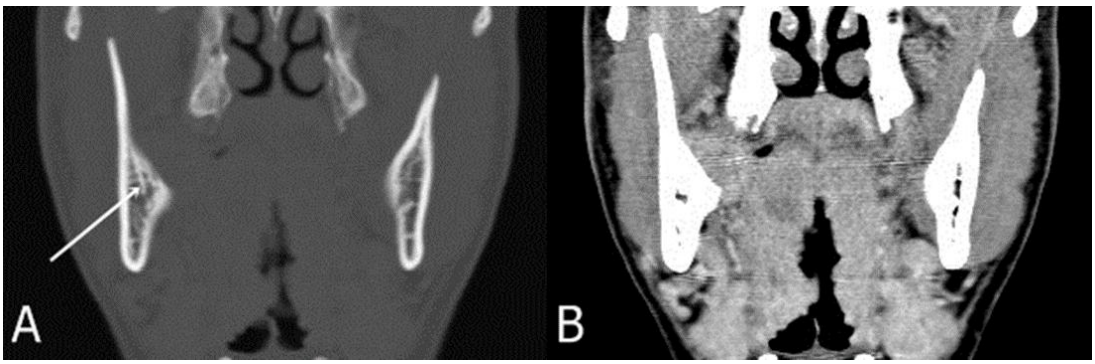

Figure 6. Coronal computed tomographic images with bone window setting (A) and soft tissue window setting (B) show subtle underlying bone sclerosis confined to the alveolar bone portion (arrow) with cortical invasion type.

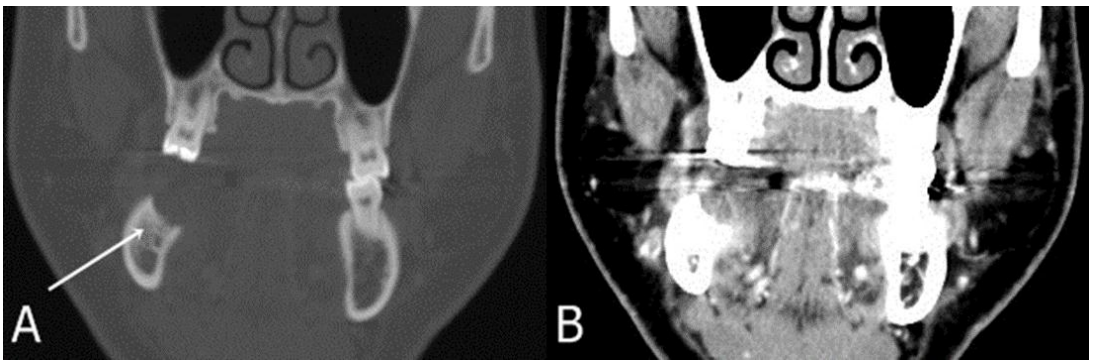

Figure 7. Coronal computed tomographic images with bone window setting (A) and soft tissue window setting (B) show prominent underlying bone sclerosis confined to the alveolar bone portion (arrow) with smooth medullary invasion type.

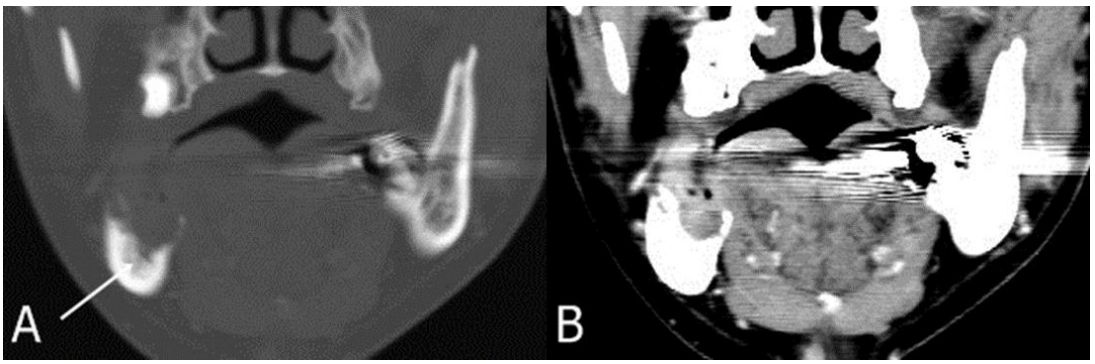

Figure 8. Coronal compute tomographic images with bone window setting (A) and soft tissue window setting (B) show prominent underlying bone sclerosis widespread to basal bone portion (arrow) with irregular medullary invasion type.

Table 3. Degree of underlying bone sclerosis (HU value) difference among groups classified by radiologic type of bone invasion

Type of bone invasion		Mean difference	Standard error	*P* value
Cortical	Medullary (smooth)	267.8*	105.1	.033
Cortical	Medullary (irregular)	407.7*	81.6	.000
Medullary (smooth)	Medullary (irregular)	140.0	105.0	.302

* $P < .05$

Table 4. Correlation of the degree of underlying bone sclerosis (HU value) with invasion depth and tumor size

Control variables			Degree of sclerosis	Invasion depth	Tumor size
None	Degree of sclerosis	Correlation		0.363*	0.370*
		P value		.001	.000
	Invasion depth	Correlation	0.363*		0.557*
		P value	.001		.000
	Tumor size	Correlation	0.370*	0.557*	
		P value	.000	.000	
Tumor Size	Degree of sclerosis	Correlation		0.203	
		P value		.064	
	Invasion depth	Correlation	0.203		
		P value	.064		
Invasion depth	Degree of sclerosis	Correlation			0.217*
		P value			.047
	Tumor size	Correlation	0.217*		
		P value	.047		

* $P < .05$

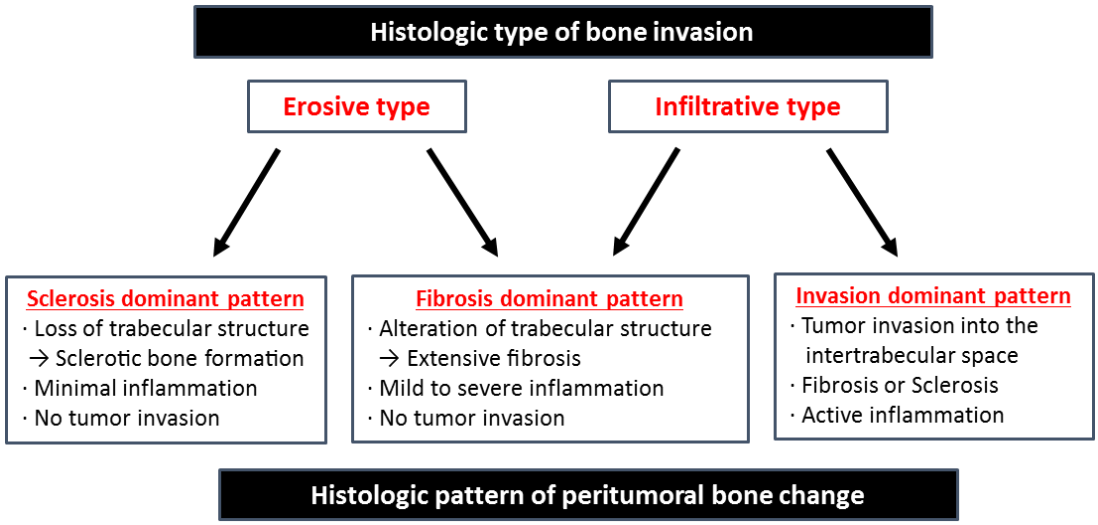

Figure 9. Histopathologic type of bone invasion and histopathologic pattern of peritumoral bone change.

Table 5. Relationship between radiologic and histopathologic findings

Radiologic findings					Histopathologic findings			
CT	MR (T1)	MR (T2)	MR (En)	PET	Type Inv	Tumor cell	Type Inv	Pattern
2	L	I	X	X	Smo	X	Inf	Scl
1	I	I	X	X	Cor	X	Ero	Scl
2	L	I	X	X	Smo	X	Ero	Scl
2	L	I	X	X	Smo	X	Ero	Scl
1	L	H	E	X	Irr	X	Inf	Fib
1	L	H	E	X	Irr	X	Inf	Fib
1	L	H	E	X	Smo	X	Ero	Fib
2	L	H	E	X	Irr	X	Ero	Fib
2	L	H	E	X	Irr	X	Inf	Fib
2	L	H	E	U	Cor	X	Inf	Fib
2	L	H	E	X	Irr	X	Ero	Fib
0	I	H	E	X	Irr	X	Inf	Fib
0	I	H	E	X	Irr	X	Inf	Fib
2	L	H	E	X	Irr	X	Inf	Fib
						O	Inf	Inv
						O	Inf	Inv
						O	Inf	Inv
						O	Inf	Inv

* Type Inv: type of invasion, Pattern: pattern of peritumoral bone change

0: no sclerosis, 1: subtle sclerosis, 2: prominent sclerosis

H: high signal intensity, L: low signal intensity, I: intermediate signal intensity

E: enhancement, U: fluorodeoxyglucose (FDG) uptake

Cor: cortical invasion type, Smo: medullary invasion with a smooth margin type, Irr: medullary invasion with an irregular margin type

Ero: erosive type, Inf: infiltrative type

Scl: sclerosis dominanat pattern, Fib: fibrosis dominant pattern, Inv: invasion dominant pattern

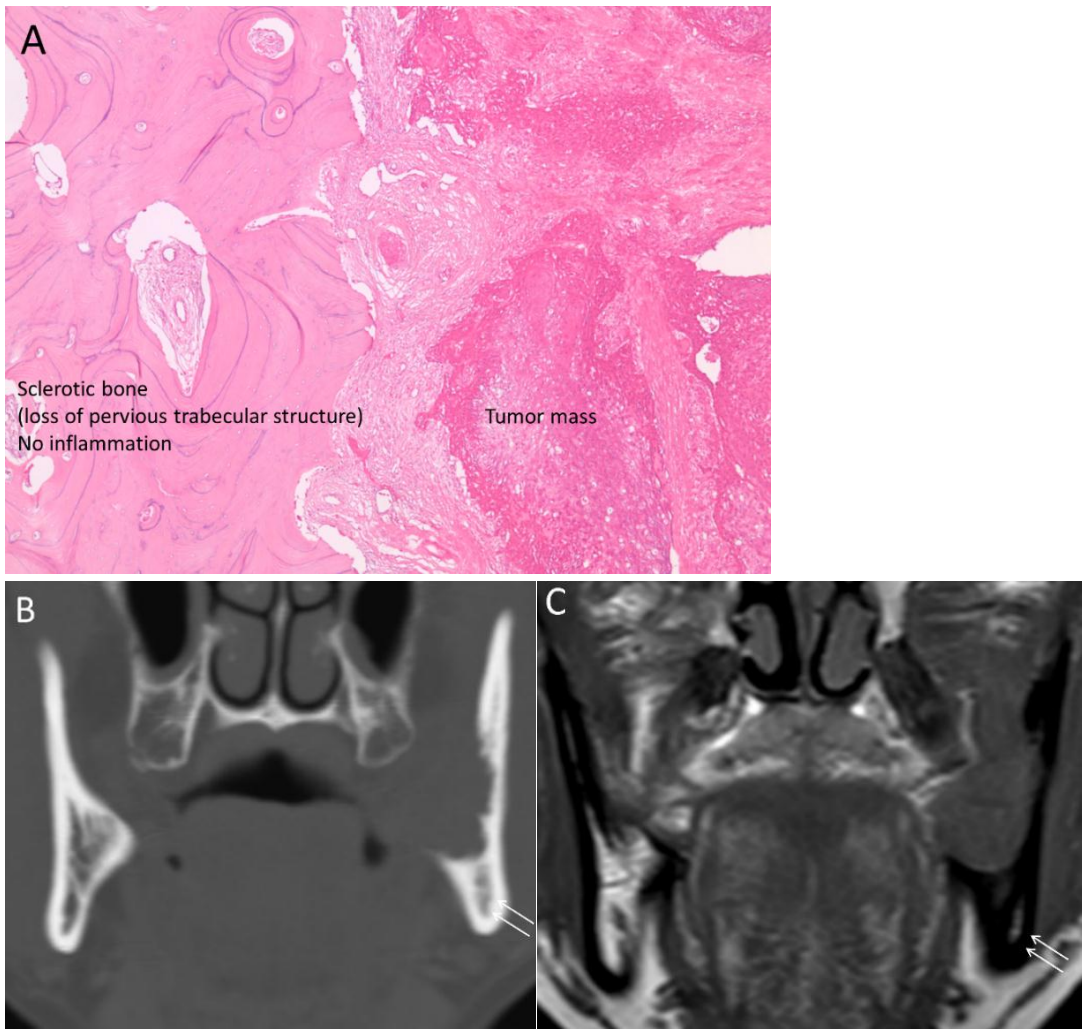

Figure 10. Erosive type of bone invasion and sclerosis dominant pattern of peritumoral bone change. (A) Photomicrograph of the histologic specimen demonstarates sclerotic bone (loss of previous trabecular structure) and no inflammation. (B) CT image with bone setting shows dense sclerosis of underlying bone (arrow). (C) T1WI shows low SI of underlying bone (arrow).

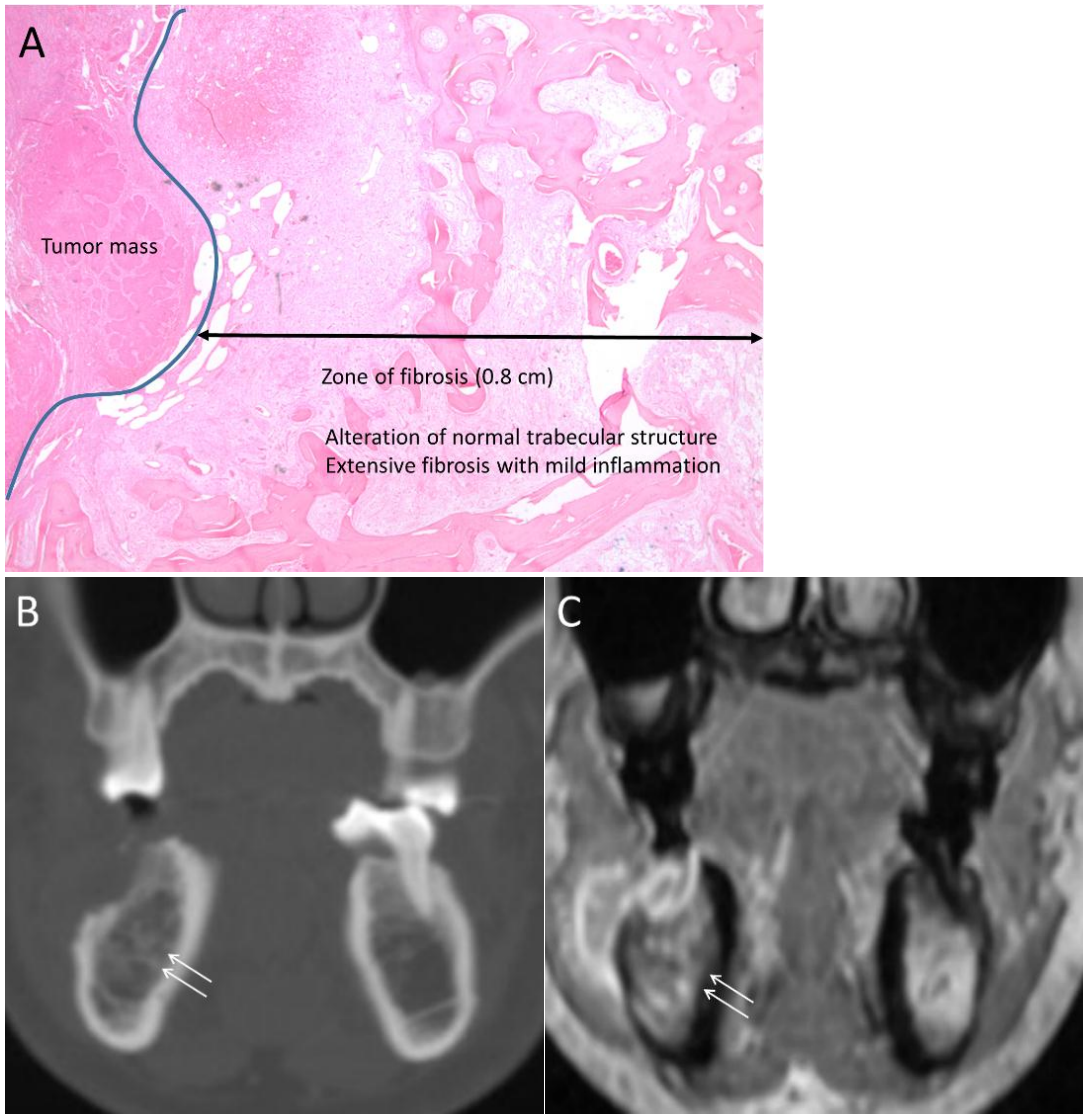

Figure 11. Erosive type of bone invasion and fibrosis dominant pattern of peritumoral bone change (A) Photomicrograph of the histologic specimen demonstarates alteration of normal trabecular structure, extensive fibrosis of bone marrow and mild inflammation. (B) CT image with bone setting shows increase attenuation of marrow space (arrow). (C) Contrast enhanced T1WI shows pathologic SI of underlying bone marrow (arrow).

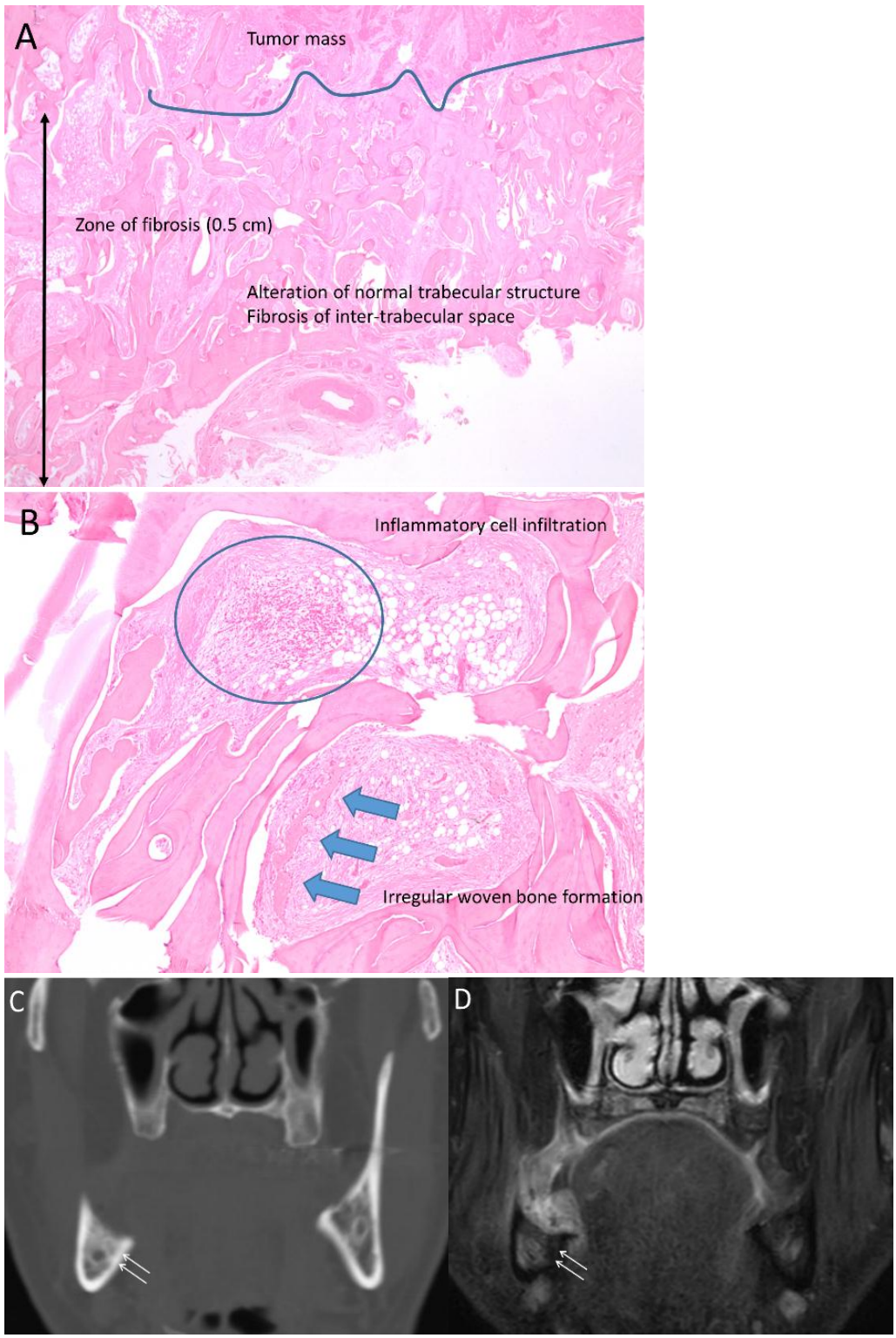
A
Tumor mass
Zone of fibrosis (0.5 cm)
Alteration of normal trabecular structure
Fibrosis of inter-trabecular space
B
Inflammatory cell infiltration
Irregular woven bone formation
C
D

Figure 12. Infiltrative type of bone invasion and fibrosis dominant pattern of peritumoral bone change. (A) Photomicrograph of the histologic specimen demonstrates alteration of normal trabecular structure, extensive fibrosis of bone marrow. (B) Photomicrograph demonstrated inflammatory cell inflammation (circle) and irregular woven bone formation (arrow). (C) CT image with bone setting shows increase attenuation of underlying bone marrow (arrow). (C) Contrast enhanced T1WI shows pathologic SI of underlying bone marrow (arrow).

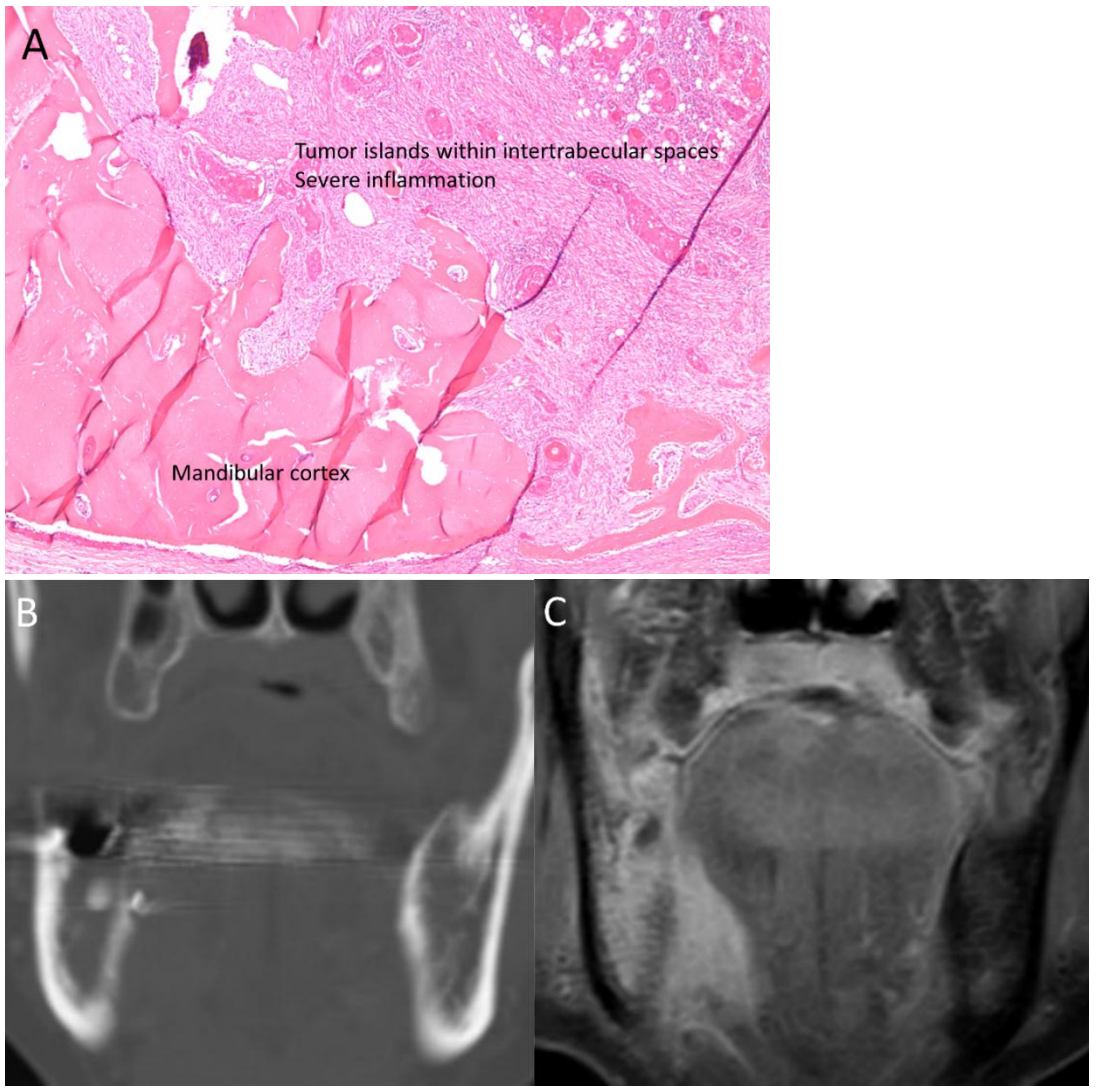

Figure 13. Infiltrative type of bone invasion and invasion dominant pattern of peritumoral bone change (A) Photomicrograph demonstrated tumor islands within intertrabecular space and severe inflammation. (B) CT image with bone setting and (C) CT image with soft tissue setting show bone destruction to the inferior cortex of the mandible and no remaining bone marrow.

IV. Discussion

Many studies have reported peritumoral change in soft tissue. For instance, intense perilesional enhancement on contrast enhanced CT and MR images has been observed for a number of hepatic metastases. And it results in indistinct outer tumor margins and overestimation of tumor size.[12] At the histopathologic examination, intense perilesional enhancement correlated with hepatic parenchymal changes, which included peritumoral desmoplastic reaction, inflammatory cell infiltration, and vascular proliferation.[12]

Similarly, in the OSCC cases where underlying bone changes are found, extent of mandibular invasion may be inappropriately overestimated, which in turn may lead to more radical resections that would not improve the prognosis. However, little is known about peritumoral change on hard tissue. To our knowledge, few studies have addressed the occurrence and possible causes of peritumoral bone change in OSCC patients. One of the previous studies with MR images reported that pathologic SI of bone marrow caused by reactive fibrous change can be seen as marrow invasion, resulting in overestimation of the tumor extent.[13] Other studies reported that MR imaging often shows similar SI in the tumor and the surrounding inflammation in the bone marrow, therefore surrounding inflammation can obscure the actual tumor margins.[14-16] However, the majority of these studies showed no histopathologic correlation.

For the cases of soft tissue resection, intraoperative frozen section analysis for margin status is possible. With the intraoperative frozen section analysis, it is possible to determine the surgical margin is clear of malignant

tumor cell or if residual malignant tumor cell is present at the surgical margin. However, such analysis is infeasible for hard tissue. Generally, in order to take section a bone sample, decalcification is essential. Therefore, a study on peritumoral change of underlying bone is necessary. Carcinoma developed in anywhere other than the oral cavity is rarely progressed to the adjacent bone. As bone invasion is commonly seen when carcinoma occurred in the oral cavity, gingival OSCC is an ideal case model to assess peritumoral change in hard tissue.

According to the histopathologic correlation, no malignant cell nest was observed in area with underlying bone change. Instead, the lesion periphery showed peritumoral bone change including thickening of trabecular bone, fibrosis of bone marrow and peritumoral inflammation. OSCC bone invasion is not a simple bone resorption by osteoclast alone. It is, rather, one of a complicated process where numerous fibroblasts, osteoblasts, and cytokines involve.[17] Tumor cell produces several cytokines such as interleukin (IL)-6 and parathyroid hormone-related protein (PTHrP). It induces fibroblast and osteoblast to synthesize a receptor activator of NF-*k*B ligand (RANKL) and it subsequently induces osteoclast formation.[18] In addition to that, osteoclast releases various growth factors such as fibroblast growth factor (FGF) during bone destruction.[19] With respect to such mechanism, it can be considered as activities of osteoblast and fibroblast also showing changes in response to tumor cell stimulation. Therefore, underlying bone change can be thought to be the result of reactive change rather than tumor cell infiltration.

In the study of margin status including 35 cases of marginal resection and 65 cases of segmental resection, the prevalence of involved margin in the soft tissue and bone were similar (3~6%), the prevalence of close margin (<5mm) was far greater in the soft tissue (33~34%) than in the bone (2~3%).[20] Further, there was not a single case in which the bone margin was compromised but the soft tissue was clear (>5mm).[20] These results suggest that the factor affecting tumor recurrence in the current situation would be soft tissue margin status rather than bone margin status. Another study revealed that, tumor size is more important than mandibular invasion in predicting local control of disease for patients with lower gingival carcinoma.[21] Considering these results, there is a possibility to try more conservative resection, marginal resection in cases of OSCC with bone invasion.

In the current study, serial section slides were prepared to verify the presence of malignant tumor cell in the region with underlying bone change. One limitation of the present study is that malignant tumor cells might be present in the region not included in the prepared serial section slides. Observing more compact interval serial section slides might raise precision. However, considering the slice thickness and interval for preoperative CT image was 2-3 mm, sectioning interval of 4 mm might be enough to investigate the radiologic-histopathologic correlation.

Lately, it has become increasingly evident that the tumor and the surrounding microenvironment are closely related and the tumor microenvironment plays a significant role in progression of the tumor in

OSCC.[22] Histopathologic type of bone invasion by OSCC is commonly categorized as erosive type and infiltrative type.[23] Conventional classification focuses on how tumor has invaded bone. However, the current study proposed the new classification called "Histopathologic pattern of peritumoral bone change" for how it responds to OSCC in terms of mandible instead of tumor. The recognition and understanding of peritumoral bone change and its distinction from true tumor mass may be important for the planning of the surgery. A better understanding of peritumoral bone change will increase our knowledge about the mechanism of bone invasion and hopefully lead to minimally invasive surgical procedure.

V. Conclusion

Underlying bone change is often accompanied by OSCC in forms of sclerosis or pathologic SI of bone marrow. It is very important to distinguish and differentiate between bone invasion by OSCC and resultant surrounding bone change. This will help to determine the bone margin of surgical resection in patients with OSCC.

VI. References

1. Warnakulasuriya S. Global epidemiology of oral and oropharyngeal cancer. Oral Oncol 2009; 45: 309-16.

2. Barasch A, Gofa A, Krutchkoff DJ, Eisenberg E. Squamous cell carcinoma of the gingiva. A case series analysis. Oral Surg Oral Med Oral Pathol Oral Radiol Endod 1995; 80: 183-7.

3. McGregor AD, MacDonald DG. Routes of entry of squamous cell carcinoma to the mandible. Head Neck Surg 1988; 10: 294-301.

4. Bark R, Mercke C, Munck-Wikland E, Wisniewski NA, Hammarstedt-Nordenvall L. Cancer of the gingiva. Eur Arch Otorhinolaryngol 2016; 273: 1335-45.

5. Byers RM, Newman R, Russell N, Yue A. Results of treatment for squamous carcinoma of the lower gum. Cancer 1981; 47: 2236-8.

6. McGregor AD, MacDonald DG. Patterns of spread of squamous cell carcinoma within the mandible. Head Neck 1989; 11: 457-61.

7. Mukherji SK, Isaacs DL, Creager A, Shockley W, Weissler M, Armao D. CT detection of mandibular invasion by squamous cell carcinoma of the oral cavity. AJR Am J Roentgenol 2001; 177: 237-43.

8. Uribe S, Rojas L, Rosas C. Accuracy of imaging methods for detection of bone tissue invasion in patients with oral squamous cell carcinoma. Dentomaxillo Rad 2013; 42: 20120346.

9. Shatzkes DR, Meltzer DE, Lee JA, Babb JS, Sanfilippo NJ, Holliday RA. Sclerosis of the pterygoid process in untreated patients with

nasopharyngeal carcinoma. Radiology 2006; 239: 181-6.

10. Dias J, Isaacs DL, Creager A, Weissler M, Mukherji SK. Mandibular sclerosis associated with squamous cell carcinoma of the oral cavity: CT-pathologic correlation. Paper presented at: 39 th Annual Metting of the American Society of Neuroradiology ; April 23-27, 2001; Boston

11. White SC, Pharoah MJ. Oral radiology: principles and interpretation. 7th ed. St. Louis: Elsevier; 2014. p. 430.

12. Semelka RC, Hussain SM, Marcos HB, Woosley JT. Perilesional enhancement of hepatic metastases: correlation between MR imaging and histopathologic findings-initial observations. Radiology 2000; 215: 89-94.

13. Imaizumi A, Yoshino N, Yamada I, Nagumo K, Amagasa T, Omura K, et al. A potential pitfall of MR imaging for assessing mandibular invasion of squamous cell carcinoma in the oral cavity. AJNR Am J Neuroradiol 2006; 27: 114-22.

14. Chung TS, Yousem DM, Seigerman HM, Schlakman BN, Weinstein GS, Hayden RE. MR of mandibular invasion in patients with oral and oropharyngeal malignant neoplasms. AJNR Am J Neuroradiol 1994; 15: 1949-55.

15. Campbell RS, Baker E, Chippindale AJ, Wilson G, McLean N, Soames JV, et al. MRI T staging of squamous cell carcinoma of the oral cavity: radiological-pathological correlation. Clin Radiol 1995; 50: 533-40.

16. Crecco M, Vidiri A, Angelone ML, Palma O, Morello R. Retromolar trigone tumors: evaluation by magnetic resonance imaging and correlation with pathological data. Eur J Radiol 1999; 32: 182-8.

17. Jimi E, Furuta H, Matsuo K, Tominaga K, Takahashi T, Nakanishi O. The cellular and molecular mechanisms of bone invasion by oral squamous cell carcinoma. Oral Dis 2011; 17: 462-8.

18. Guise TA, Mundy GR. Cancer and bone. Endocr Rev 1998; 19: 18-54.

19. Partridge M, Kiguwa S, Luqmani Y, Langdon JD. Expression of bFGF, KGF and FGF receptors on normal oral mucosa and SCC. Eur J Cancer B Oral Oncol 1996; 32B: 76-82.

20. Brown J. Mechanisms of cancer invasion of the mandible. Curr Opin Otolaryngol Head Neck Surg 2003; 11: 96-102.

21. Overholt SM, Eicher SA, Wolf P, Weber RS. Prognostic factors affecting outcome in lower gingival carcinoma. Laryngoscope 1996; 106: 1335-9.

22. Hanahan D, Weinberg RA. Hallmarks of cancer: the next generation. Cell 2011; 144: 646-74.

23. Wong RJ, Keel SB, Glynn RJ, Varvares MA. Histological pattern of mandibular invasion by oral squamous cell carcinoma. Laryngoscope 2000; 110: 65-72.

요약(국문초록)

구강편평세포암종의 주변 골 변화: 영상 특성 및 조직병리학적 상관관계 분석

조규동

서울대학교 대학원

치의과학과 영상치의학 전공

(지도교수 허경회)

목적

구강편평세포암종이 하악골을 침범할 때, 그 주위로 전산화단층촬영 영상에서 골 경화성 반응 혹은 자기공명영상에서 골수조직의 병적 신호강도가 자주 관찰되고, 이것은 악성 종양세포의 악골 침범 범위를 결정하는 데 혼란을 준다.

이 연구의 목적은, 하악골 침범을 보이는 구강편평세포암종 환자를 대상으로 1) 술전 전산화단층촬영, 자기공명 영상에서 관찰되는 주변 골 변화의 빈도를 조사하고, 2) 주변 골 변화와 종양의 공격성 간의 상관관계를 밝히며, 3) 주변 골 변화 부위를 영상-조직병리 상관관계 분석을 통해 조직 슬라이드 상에서 분석해 보는 것이다.

재료 및 방법

이 연구는 2009 년 9 월부터 2016 년 12 월까지 구강편편세포암종 치료를 위해 하악골 절제술을 시행한 137 개 증례를 대상으로 한다. 술전 전산화단층촬영, 자기공명 영상에서 관찰되는 주변 골 변화의 빈도를 두 명의 영상치의학 전문의가 평가하였다. 또한 이러한 주변 골 변화와 영상학적 특징들(악골 침범 양상, 악골 침범 깊이, 악성 병소의 크기), 조직병리학적 특징들(TN 병기, 세포분화도), 임상적 특징(재발 여부)과의 상관관계를 분석하였다.

2016 년 1 월 이후에 하악골 절제술을 시행한 18 개 증례들을 대상으로, 절제된 종물의 연속 절편 슬라이드를 제작하였고 한 명의 독립된 구강병리학 전문의가 조직병리 슬라이드 상에서 주변 골 변화 부위를 분석하였다. 조직병리학적 특징들(악성 종양 세포의 침범 유무, 해면골 구조의 변화, 골수 조직의 섬유화, 염증세포의 침윤)을 평가하였고, 이를 바탕으로 주변 골 변화 유형을 분류하였다.

결과

술전 영상 분석에서, 69.6%의 증례가 전산화단층촬영영상에서 주변 골의 골경화성 반응을 보였고 90.9%의 증례가 자기공명영상에서 골수조직의 병적 신호강도를 보였다. 주변 골 변화를 보인 증례들은 유의하게 더 침습적인 악골 침범 양상, 더 깊은 악골 침범 깊이, 더 큰 악성 병소 크기를 보였다.

조직병리학적으로 주변 골 변화는 3 가지 유형(4 개 증례 의 골경화 우세형, 10 개 증례의 골수섬유화 우세형, 4 개 종류의 악성 세포 침윤 우세형)으로 분류할 수 있었다. 골경화 우세형과 골수섬유화 우세형으로 분류된 증례들은

술전 영상에서 주변 골 변화를 보였지만, 조직병리 슬라이드에서 그 부위로의 악성 종양 세포의 침윤은 관찰되지 않았다.

결론

구강편평세포암종은 하악골을 침범할 때 골 경화성 반응이나 골수 조직의 병적 신호강도 형태의 주변 골 변화를 자주 동반한다. 구강편평세포암종의 골 침범과 그 주변 골의 병적 변화를 정확히 구분하고 감별하는 것은 매우 중요하다. 이것은 구강편평세포암종 환자에서 하악골 절제 범위를 적절히 설정하는데 도움을 줄 것으로 생각한다.

주요어: 편평상피세포암, 하악골, 전산화단층촬영 영상, 자기공명 영상
학 번: 2015-31271